METHODOLOGICAL NOTES

Quantum corrections to the equilibrium rate constants of inelastic processes

A V Eletskiĭ, A N Starostin, M D Taran

Contents

Abstract. The quantum corrections which the equilibrium rate constants of inelastic processes acquire due to particle momenta deviating from the Maxwell distribution at high gas pressures and relatively low temperatures are considered. This deviation can be interpreted as a manifestation of the time-energy uncertainty relation for particles colliding elastically at a high rate, with the characteristic energy $\sim \hbar v$ (where v is the collision frequency) put into correspondence with the temperature. Taking account of this deviation changes the temperature dependences of the rate constants of adiabatic and exothermal processes, as illustrated by the examples of vibrationally relaxing diatomic molecules and nuclear fusion and chemical processes. The experimental anomalies in the temperature dependences of the corresponding rate constants are accounted for adequately by introducing the non-Maxwellian corrections.

1. Introduction

As is well known, the rate constants of many exothermic chemical reactions as well as adiabatic processes at low temperatures are characterized by a sharply increasing temperature dependence. The existence and the shape of the dependence mentioned determine the character of such

A V Eletskiĭ Russian Research Centre 'Kurchatov Institute',
pl. Kurchatova 1, 123182 Moscow, Russian Federation
Tel./Fax (7-095) 196 72 80
E-mail: eletskii@imp.kiae.ru
A N Starostin, M D Taran RF State Scientific Center
'Troitsk Institute for Innovation and Fusion Research',
142190 Troitsk, Moscow region, Russian Federation
Tel./Fax (7-095) 334 51 58. Tel. (7-095) 196 98 40
E-mail: staran@triniti.ru

important phenomena as the transition of combustion into detonation, flame propagation, vibrational relaxation, and even thermonuclear fusion. In the case of exothermic reactions, such a dependence can be caused by the threshold character of the reaction and occurs when the gas temperature T is much less than the characteristic threshold reaction energy ΔE. In the case of adiabatic processes, whose condition of occurrence is the criterion $b\Delta E/\hbar v \gg 1$ (b is the characteristic length of intermolecular forces, and v is the collision velocity), the reason for a sharp temperature dependence of the rate constant of the process relates to a sharp exponential increase in the probability of the process under consideration as the collision velocity rises. In both cases, the specific shape of the temperature dependence of the process rate constant is governed by the behavior of the particle kinetic energy distribution function at energies considerably exceeding the gas temperature or as the saying goes 'on the tail of the Maxwellian distribution'. For a rarefied gas, the equilibrium shape of the particle kinetic energy distribution function is described by the Maxwellian exponent

$$f(\varepsilon) \sim \exp\left(-\frac{\varepsilon}{T}\right) \tag{1}$$

(ε is the kinetic energy of a particle). This leads to the well-known 'Arrhenius' temperature dependence

$$k \sim \exp\left(-\frac{\Delta E}{T}\right) \tag{2}$$

for the rate constant of many exothermic processes, and to the Landau – Teller type dependence

$$k \sim \exp\left[-\left(\frac{T_0}{T}\right)^{1/3}\right] \tag{3}$$

for an adiabatic exothermic process (here, $T_0 \gg T$ is the parameter depending on the properties of colliding particles).

At an enhanced pressure, however, the particle kinetic energy distribution function on a high-energy 'tail' can differ notably from the simple exponential dependence (1). As first noted by Galitskiĭ and Yakimets [1], this difference is caused by the quantum uncertainty of the particle energy at a high collision frequency, which is a peculiar kind of particle spectral line broadening (see below). This 'tail' phenomenon is inherent to the particle momentum distribution function and is similar to the Lorentz asymptotic behavior of a spectral line against the background of the Doppler kernel. However, as distinguished from the purely classic treatment of the spectral line profile, the power-like 'tail' of the particle momentum distribution function has an essentially quantum origin, because the equilibrium particle momentum distribution function remains Maxwellian in classical statistics independently of both the gas density and interaction potential between particles due to the commutability of kinetic and potential energies. Owing to this effect, the exponentially decreasing momentum (or kinetic energy) distribution function is supplemented with an item which decreases more slowly, in a power-like manner, as the kinetic energy rises. The power index of this function is determined by the energy dependence of the elastic scattering cross section in the energy region making the main contribution to the formation of the particle energy distribution function. The relative contribution of the nonexponential item to the particle energy distribution function increases with a rise in the number density of colliding particles, because it results in a rise in the collision frequency, and with a decrease in the temperature, because the exponential function drops more rapidly with the temperature than the power-like one. Taking into account the nonexponential addition to the particle momentum distribution function at relatively high pressures and low temperatures results in notable changes in temperature dependences of the rate constants of adiabatic and exothermic processes compared to the classic expressions (2) and (3).

In parallel with the interpretation based on the time–energy uncertainty relation, the effect of 'nonexponential tail growing' can also be treated in terms of the coordinate–momentum uncertainty relation. According to this treatment, the interaction of a particle with its surroundings restricts the volume of configuration space, which, due to the uncertainty relation, results in an increase in the volume of the momentum space, i.e., in a rise in the fraction of particles with higher momenta. Two ways of interpreting the influence of power-like 'tails' on the momentum distribution function can be interconnected using the relation $\hbar v/T \sim \lambda_T/l$, where λ_T is the thermal de Broglie wavelength of a particle, and l is its mean free path with respect to a change in its momentum. The Lorentz gas model will be considered below in the limiting case of $\lambda_T/l \ll 1$. The theory is highly sophisticated with the proviso that $\lambda_T/l \sim 1$, so that the Anderson localization becomes possible.

The quantum corrections to the particle momentum distribution function are evaluated in the present work in the framework of a model approach. Considering several examples of processes of such a type, it will be shown that taking into account the quantum corrections to the equilibrium particle momentum distribution function allows at least a qualitative explanation of some experimentally examined anomalies in temperature dependences of the rate

constants of vibrational relaxation of molecules, thermonuclear fusion reactions, and exothermic chemical reactions determining the spontaneous combustion time for the oxygen–hydrogen mixture.

2. Particle momentum distribution function including the quantum correction

The generalized distribution function of particles over energies E and momenta p has the form

$$f(E, \mathbf{p}) \equiv \int \exp\left(iE\tau - i\mathbf{p}\mathbf{r}\right) < \Psi^*(x_2)\,\Psi(x_1) > d\tau\,d\mathbf{r}. \quad (4)$$

Here, $x = (\mathbf{r}, t)$, $\tau = t_1 - t_2$; $\mathbf{r} = \mathbf{r}_1 - \mathbf{r}_2$, and $\Psi(x)$ is the field operator of a particle in the Heisenberg representation. As is shown in Ref. [2], the following analytical expression is arrived at:

$$f(E, \mathbf{p}) = n(E)\,\frac{\gamma(E, \mathbf{p})}{\pi\left[\left(E - \varepsilon_p - \Delta(E, \mathbf{p})\right)^2 + \gamma^2(E, \mathbf{p})\right]}$$
$$\equiv n(E)\,\delta_\gamma(E - \varepsilon_p), \quad (5)$$

where $n(E)$ is the occupation number. In particular, for electrons in the thermodynamically equilibrium state, one has

$$n(E) = \frac{1}{\exp\left[(E - \mu)/T\right] + 1}, \quad (6)$$

where μ is the chemical potential, T is the temperature, $\varepsilon_p = p^2/2m$ is the kinetic energy, $\gamma \sim \hbar v$ is the collision width, v is the collision frequency, and Δ is the density energy shift. The particle momentum distribution function is derived by integrating relationship (5) over the energy:

$$f(\mathbf{p}) = \int dE\, f(E, \mathbf{p}). \quad (7)$$

Specifically, in a rarefied gas the collision width γ of the spectral function $\delta_\gamma(E - \varepsilon_p)$ is negligible; therefore, the Lorentzian in formula (5) operates like the δ function. This results in the following expression

$$f(\mathbf{p}) = \exp\left(\frac{\mu}{T}\right)\exp\left(-\frac{\varepsilon_p}{T}\right) \quad (8)$$

which corresponds to the classical, Maxwellian particle momentum distribution function. In the case of a moderate-density gas, the expression for the particle momentum distribution function contains the power-like correction along with the resonant, Maxwellian dependence (8) in a high-energy region $\varepsilon_p \gg \{T, \gamma, \Delta\}$:

$$f(\mathbf{p}) = \frac{1}{\pi\varepsilon_p^2}\int_{-\infty}^{\infty} n(E)\,\gamma(E, \mathbf{p})\,dE. \quad (9)$$

Relatively simple expressions for the quantum correction to the particle momentum distribution function can be derived in the framework of the Lorentz gas model, where the motion of a diluted admixture of light particles with the concentration n in a heavy particle gas of concentration N is considered [3]. In this case, the quantity $\gamma(E, \mathbf{p})$ is determined from the following approximate integral equation that is used in the

theory of metals:

$$\gamma(E, \mathbf{p}) = \frac{\pi N}{\hbar^3} \int \left| U(\mathbf{p} - \mathbf{p}_1) \right|^2 \delta_\gamma (E - \varepsilon_{p_1}) \, \frac{\mathrm{d}^3 \mathbf{p}_1}{(2\pi)^3} \,. \tag{10}$$

Here, the quantity $\Delta(E, \mathbf{p})$ is given as follows:

$$\Delta(E, \mathbf{p}) = \mathrm{P} \int \frac{\gamma(E, \mathbf{p})}{k - E} \, \mathrm{d}k + \sum{}^{\mathrm{HF}}(E, \mathbf{p}) \,, \tag{11}$$

where $U(\mathbf{q})$ is the Fourier transform of the interaction potential between a particle and an admixture, P is the symbol of the principal integral value, and $\sum^{\mathrm{HF}}$ is the Hartree–Fock contribution to the particle energy shift. The parameter γ can be estimated approximately on the basis of relationship (10):

$$\gamma(E, p) = \frac{\hbar N}{2} \, \sigma_{\mathrm{t}} \big[p, p_1(E) \big] \sqrt{\frac{2E}{m}} \,. \tag{12}$$

This estimation fits with the meaning of the parameter $\gamma \sim \hbar v$ as a quantity proportional to the elastic collision frequency. Indeed, the Born approximation gives the following expression for the total scattering cross section [4]:

$$\sigma_{\mathrm{t}} = \int \mathrm{d}\Omega \, \frac{m^2}{4\pi^2 \hbar^4} \left| \int \mathrm{d}\mathbf{r} \, U(r) \exp\left(-\mathrm{i}\mathbf{q}\mathbf{r} \right) \right|^2 \,, \tag{13}$$

where $\mathbf{q} = \mathbf{p} - \mathbf{p}_1$, and $p_1 = (2mE)^{1/2}$.

At high momenta ($\varepsilon_p \gg T$), the quantity $f(p)$ is defined by the following asymptotic expression that is derived from formulas (7)–(13):

$$f(p) = \exp\left(\frac{\mu}{T} \right) \left[\exp\left(-\frac{\varepsilon_p}{T} \right) + \frac{\hbar N T \sigma_{\mathrm{t}}(p)}{2\pi \varepsilon_p^2} \sqrt{\frac{\pi T}{2m}} \right] \,. \tag{14}$$

The second term in square brackets presents the sought-for quantum correction to the particle momentum distribution function, which is caused by collisions. As can be seen, the relative contribution of this correction will be enhanced as the density of particles increases and the temperature decreases, so that it can become determining in some conditions. For example, in the case of the electron gas for which $\sigma_{\mathrm{t}} \sim \varepsilon_p^{-2}$ having regard to the Debye screening, this correction depends on the momentum as $\sim p^{-8}$ [1]. Note that the Born approximation for electrons is valid at high ε_p.

The expression for the rate constant of an inelastic process $i \to j$ accompanied by the energy release (energy absorption) $\pm I$ can be derived within the framework of the same Lorentz gas model [3]:

$$nk_{ij} = A \iint \mathrm{d}\mathbf{p} \, \mathrm{d}\mathbf{p}' \int_{-\infty}^{\infty} \mathrm{d}E \left| f_{ij}(\mathbf{p}, \mathbf{p}') \right|^2 \delta_\gamma(E - \varepsilon_p)$$
$$\times \, \delta_\gamma(E \pm I - \varepsilon_{p'}) \, n(E) \big[1 - n(E \pm I) \big] \,. \tag{15}$$

Here, A is the normalization factor that can be evaluated by fitting the expression for k_{ij} in the limiting case $\gamma \to 0$ with its classical value, and f_{ij} is the scattering amplitude for the process $i \to j$ outside the mass surface. This amplitude depends on the center-of-mass momenta before and after inelastic collision, which are not interconnected with each other by the kinetic energy conservation law: $\varepsilon_p' \neq \varepsilon_p \pm I$ at a finite value of γ. Relation (15) is valid for $I \gg \gamma$. In the gas approximation, the amplitude f_{ij} does not depend on the density of the medium.

Expression (15) implies that for a relatively low temperature $T \ll I$ the rate of a reaction with the absorption of the energy ('−' sign) is exponentially low $\left[\sim \exp\left(-I/T \right) \right]$. This case is described by the exponential temperature dependence both in the classical limit $\gamma \to 0$ and at a finite value of the parameter γ. In the former case, this follows from Eqn (15) taking into account the kinetic energy conservation law and using the δ function as $\gamma \to 0$. At a finite value of the parameter γ, the integration in formula (15) over E is not limited by the region $E > I$, so that the exponentially low value of the rate constant of an endothermic process is caused by a low magnitude of the last factor in square brackets in Eqn (15). One should stress that the magnitudes of the rate constant in two cases can differ considerably.

In the case of processes with the energy release ('+' sign in Eqn (15) or for exothermic reactions), the above-mentioned factor that presents, for example, the Pauli blockage effect for electrons is practically equal to unity. Taking into account these circumstances, equation (15) is simplified considerably, which has been confirmed by numerical calculations. Having regard to the known relationship [4]

$$\mathrm{d}\sigma_{ij} = \frac{p'}{p} \left| f_{ij}(p, p') \right|^2 \mathrm{d}\Omega \,, \tag{16}$$

and also to a weak dependence of σ_{ij} on p' (see below), the integration of the second Lorentzian in formula (15) over $\mathrm{d}\mathbf{p}'$ results in unity. This leads to the following equation which is a generalization of the classical definition, taking into consideration the quantum corrections:

$$nk_{ij} = A' \int \mathrm{d}\mathbf{p} \, f(\mathbf{p}) \left(\frac{p}{m} \right) \bar{\sigma}_{ij}(p) \,. \tag{17}$$

Relation (17) defines the rate constant $k_{ij} = \langle \sigma_{ij} v \rangle$ of the process under discussion through the total particle momentum distribution function $f(\mathbf{p})$. The function $\sigma_{ij}(p)$ can be evaluated by solving the quantum scattering problem, so that the cross section is determined generally by the scattering amplitude outside the mass surface [see Eqns (15), (16)]. The asymptotic form (14) can be used for the total particle momentum distribution function $f(\mathbf{p})$ entering expression (17). Due to the detailed balance principle, a rise in the rate constant of an exothermic process results in an increase in the reverse (endothermic) reaction rate, although this reaction, as was noted, contains the exponential temperature dependence. The equilibrium constant which interconnects the rate constants of direct and reverse reactions is determined by thermodynamics, and varies only slightly within the framework of our weakly nonideal gas (or plasma) approach taking into account the quantum corrections to the particle momentum distribution function.

Relations (14) and (17) were derived within the context of the Lorentz gas model, when the mass of a scattered particle is small compared to that of an excited target, and they often collide with motionless admixture particles, i.e. this model implies that there is no disparity between the particle momenta in lab coordinates and the relative momenta of light and heavy particles. These relations can also be used for the description of the collision of particles with comparable masses in the first approximation, assuming that the quantity p in formula (17) is the relative momentum of colliding particles and substituting the reduced mass μ for the mass m in Eqn (14), so that $\varepsilon_p = p^2/2\mu$. This approximate approach is justified qualitatively in Section 5.

As shown below, the considered quantum correction to the rate constant of an inelastic collision process involving heavy particles can play a notable role in the case of the vibrational relaxation of diatomic molecules at temperatures around room temperature and pressures around or higher than atmospheric. Taking account of this correction smooths the temperature dependence of the vibrational relaxation rate constant of molecules in a low-temperature and high-pressure regions and results in an increasing dependence of the rate constant on the gas pressure. In addition, the inclusion of the quantum correction changes the character of the temperature dependence of threshold exothermic chemical reactions and processes characterized by a high energy barrier, e.g., thermo-nuclear fusion.

3. Amplitude of an inelastic VT collision outside the mass surface

The vibrational relaxation (VT relaxation) resulting in the transformation of the vibrational energy of a molecule into translational energy presents one of the typical examples of adiabatic processes for which the quantum correction can be essential. The rate constant of the vibrational relaxation of diatomic molecules at temperatures on the order of or higher than room temperature is characterized by an extraordinarily sharp temperature dependence [5–7]. This is caused by the adiabatic character of the vibrational relaxation process, for which reason the collisional relaxation probability depends in an exponential manner on the Massey parameter

$$\mathrm{Me} \sim \frac{b\omega}{v} \sim \frac{b\mu^{1/2}}{m^{1/2}T^{1/2}} \, . \tag{18}$$

In this relation expressed in Hartree atomic units, $b \sim 1$ is the characteristic range of intermolecular forces, $\omega \sim m^{-1/2}$ is the molecular vibration frequency, m is the reduced mass of the molecule, $v \sim (T/\mu)^{1/2}$ is the collision velocity, and μ is the reduced mass of the colliding pair. As can be seen, on condition that $m/\mu \sim 1$, which obeys for the majority of diatomic molecules, except hydrogen halides, the magnitude of the Massey parameter $\mathrm{Me} \sim T^{-1/2} \gg 1$ over the whole temperature range of practical interest. This results in the sharply increasing velocity dependence of the probability of VT relaxation, established first by Landau and Teller [5]:

$$P_{\mathrm{VT}}(v) \sim \exp\left(-c\mathrm{Me}\right) = \exp\left(-\frac{cb\omega}{v}\right) \ll 1 \, , \tag{19}$$

where c is a dimensionless numerical factor on the order of unity.

Averaging dependence (19) over the Maxwellian particle velocity distribution function gives the temperature dependence of the rate constant of the process under consideration:

$$k_{\mathrm{VT}} \sim \exp\left[-\left(\frac{T_0}{T}\right)^{1/3}\right] , \tag{20}$$

which is known as the Landau – Teller formula. Here, T_0 is a parameter, the value of which considerably exceeds room temperature for the majority of diatomic molecules. Dependence (20) is inherent to many molecular systems at temperatures exceeding room temperature. However, this dependence is not followed at reduced temperatures, so that the vibrational relaxation rate constant can exceed by many times that determined by the Landau – Teller formula (20). One of the origins of such a deviation relates to the role of the long-range van der Waals attraction of molecules, for which reason the collision energy of molecules cannot take an arbitrarily low magnitude [7].

Another factor affecting the temperature dependence of the vibrational relaxation rate constant and manifesting itself at high gas pressures relates to the role of many-particle effects [8–10]. This factor, which is also most notable at temperatures lower than or around room temperature, plays an essential role at $Nb^3 \sim 1$ (N is the number density of gas particles, and b is the characteristic range of intermolecular forces). The relevant corrections arise, particularly, as a result of taking into account the density dependence of the scattering amplitude in Eqns (15)–(17), the dependence originated from many-body collisions.

One more mechanism that is capable of considerably changing the character of the temperature dependence of the vibrational relaxation rate constant of diatomic molecules at high pressures and relatively low temperatures relates to the quantum effects under consideration, which lead to a deviation in the particle momentum distribution function from the Maxwellian one. The VT relaxation rate constant taking this mechanism into consideration can be evaluated by averaging the cross section of this process over the above-found particle velocity distribution function (14).

The quantum problem on the energy exchange between an excited oscillator having mass M and an oscillation frequency ω and a structureless particle of mass m has been resolved by Jackson and Mott [11] within a one-dimensional approach. This solution will be used further for determining the scattering amplitude $f_{ij}(\mathbf{p}, \mathbf{p}')$ outside the mass surface that is engaged in formula (15). The interaction potential between the oscillator and the incident particle will be approximated by the exponential dependence

$$V(x, X) = C \exp\left[-a(x - X)\right] , \tag{21}$$

where X is the coordinate of the oscillator being found in the initial nth state characterized by the wave function $\psi_n(X)$, and x is the coordinate of the incident particle. We represent the wave function of the colliding particles through the standard expansion

$$\Psi(x, X) = \sum_n \psi_n(X) f_n(x) . \tag{22}$$

Denoting the initial state of the oscillator by index i, and the final one by n, one obtains the following standard asymptotic (for large x) representation for the scattered particle wave function:

$$f_i(x) \sim \exp\left(-ik_ix\right) + A_i \exp\left(ik_ix\right) , \tag{23a}$$

$$f_n(x) \sim A_n \exp\left(ik_nx\right) . \tag{23b}$$

Here, $k_i = mv_i/\hbar$, and the initial v_i and the final v_n velocities are interconnected with each another through the energy conservation law: $mv_n^2/2 = mv_i^2/2 + \hbar\omega$.

The solution of the given problem within the framework of the distorted-wave Born approximation has the following form [11] (neglecting an unessential phase factor):

$$A_n = \frac{2Y_{in}}{k_n} \int_{-\infty}^{\infty} U(x) F_n(x) F_i(x) \, dx . \tag{24}$$

Here, the notation was adopted:

$$U(x) = \frac{2mC}{k_n} \exp{(-ax)}, \qquad (25)$$

$$Y_{ns} = \int \exp{(aX)} \, \psi_n(X) \, \psi_s(X) \, dX. \qquad (26)$$

Due to the small amplitude of nuclear vibrations in molecules ($aX \ll 1$), the magnitude of integral (26) at $s = n$ is close to unity. Note that $F_n(x)$ are the eigenfunctions for the scattering equation in the exponential potential (25):

$$\left[\frac{d^2}{dx^2} + k_n^2 - U(x) \right] F_n(x) = 0. \qquad (27)$$

The 3D representation of the scattering amplitude outside the mass surface for the inelastic scattering of a particle of mass m by an atomic particle having internal degrees of freedom has the following form

$$f_{i \to n}(\mathbf{p}_i, \mathbf{p}')$$
$$= -\frac{m}{2\pi\hbar^2} \int \exp{(-i\mathbf{p}'\mathbf{r})} \, \Psi_n^*(\mathbf{R}) \, V(\mathbf{r}, \mathbf{R}) \, \Psi_i(\mathbf{r}, \mathbf{R}) \, d\mathbf{r} \, d\mathbf{R}, \quad (28)$$

where $\Psi_i(\mathbf{r}, \mathbf{R})$ is the total wave function of the system involving the incident particle with an initial momentum $\mathbf{p}_i$ and the atomic system in the state $\Psi_i(\mathbf{R})$. Using the Schrödinger equation for the total wave function $\Psi_i(\mathbf{r}, \mathbf{R})$, one can exclude the interaction potential $V(\mathbf{r}, \mathbf{R})$ from relationship (28):

$$f_{i \to n}(\mathbf{p}_i, \mathbf{p}') = -\frac{1}{4\pi} \left[p_i^2 - p'^2 + (E_i - E_n) \frac{2m}{\hbar^2} \right]$$
$$\times \int \exp{(-i\mathbf{p}'\mathbf{r})} \, \Psi_n^*(\mathbf{R}) \, \Psi_i(\mathbf{r}, \mathbf{R}) \, d\mathbf{r} \, d\mathbf{R}. \qquad (29)$$

Designating the final state momentum by p_n brings this equation to the following form

$$f_{i \to n}(\mathbf{p}_i, \mathbf{p}') = \frac{1}{4\pi} (p'^2 - p_n^2)$$
$$\times \int \exp{(-i\mathbf{p}'\mathbf{r})} \, \Psi_n^*(\mathbf{R}) \, \Psi_i(\mathbf{r}, \mathbf{R}) \, d\mathbf{r} \, d\mathbf{R}. \qquad (30)$$

The total wave function of the system is represented within the framework of the distorted-wave approximation as follows:

$$\Psi_i(\mathbf{r}, \mathbf{R}) = \Psi_i(\mathbf{R}) f_i(\mathbf{r}) + \Psi_n(\mathbf{R}) f_n(\mathbf{r}). \qquad (31)$$

Substituting expression (31) into Eqn (30) results in

$$f_{i \to n}(\mathbf{p}_i, \mathbf{p}') = \frac{1}{4\pi} (p'^2 - p_n^2) \int \exp{(-i\mathbf{p}'\mathbf{r})} f_n(\mathbf{r}) \, d\mathbf{r}. \qquad (32)$$

Since the problem in the original formulation of Jackson and Mott is a one-dimensional one, integral (32) should also be calculated in the 1D case, having regard to expression (24) for the amplitude. Taking into consideration the asymptotic behavior of the function f_n [see expression (23b)], one obtains

$$f_{i \to n}(p_i, p') = \frac{p' + p_n}{2p_n} \exp{(-i\eta)} \, A_n(p_i, p_n), \qquad (33)$$

where η is a phase unessential for further analysis. Using the standard definition of the transition probability [4]

$$P_{i \to n} = \frac{p_n}{p_i} \left| A_n(p_i, p') \right|^2, \qquad (34)$$

we obtain

$$\left| f_{i \to n}(p_i, p') \right|^2 = \left(\frac{p' + p_n}{2p_n} \right)^2 \frac{p_i}{p_n} \, P_{i \to n}. \qquad (35)$$

The dependence of the scattering amplitude of an inelastic process outside the mass surface on p' is seen to be determined mainly by the factor $[(p' + p_n)/2p_n]^2$, and is rather weak, which is in accordance with the comments made in the Introduction. The expression for the transition probability is derived as a result of the exact solution to equation (27) and integration in formula (24) [11]:

$$\left| f_{i \to n}(p_i, p') \right|^2 = \left(\frac{p' + p_n}{2p_n} \right)^2 \frac{p_i}{p_n} \frac{8\pi}{\hbar^2} \frac{m}{M} \frac{m\hbar\omega}{a^2}$$
$$\times \frac{\sinh{(\pi q_i)} \sinh{(\pi q_n)}}{\left[\cosh{(\pi q_i)} - \cosh{(\pi q_n)} \right]^2}, \qquad (36)$$

where the dimensionless parameters $|q| \gg 1$ are interconnected with the wave vector k by the following relations

$$q_n = \frac{2k_n}{a}, \qquad q_i = \frac{2k_i}{a}. $$

Due to the condition $|q| \gg 1$, the expression for the vibrational relaxation rate constant in the one-dimensional formulation takes the following form [cf. formula (15)]:

$$nk_{i \to n} = A \int dE \, n(E) \left[1 - n(E + \hbar\omega) \right]$$
$$\times \int dp \, dp' \, \delta_\gamma(E - \varepsilon_p) \, \delta_{\gamma'}(E - \varepsilon_{p'} + \hbar\omega)$$
$$\times \left(\frac{p' + p_n}{2p_n} \right)^2 \frac{p}{p_n} \exp{[\pi(q_i - q_n)]}. \qquad (37)$$

The last factor in expression (37) can be rewritten as follows

$$\exp{[\pi(q_i - q_n)]} = \exp{\left(\pi \frac{q_i^2 - q_n^2}{q_i + q_n} \right)} = \exp{\left(-\frac{2\pi\omega}{a\bar{v}} \right)}, \qquad (38)$$

where

$$\bar{v} = \frac{1}{2} \left[\sqrt{\frac{2\varepsilon_p}{m}} + \sqrt{\frac{2(\varepsilon_p + \hbar\omega)}{m}} \right]. \qquad (39)$$

4. Estimation of the VT relaxation rate constant in a dense media with due regard for the effects of the quantum energy uncertainty

Expression (37) is reduced to a more simple analytical form introducing the following designations for the characteristic temperatures of molecules:

$$\theta' = \frac{m}{2} \left(\frac{\pi\omega}{a} \right)^2, \qquad \theta = \hbar\omega. \qquad (40)$$

Some further simplifications have resulted in the following form of Eqn (37):

$$nk_{VT} = A \exp\left(\frac{\mu}{T}\right)$$

$$\times \left\{ \int_0^\infty \frac{dE}{E + \hbar\omega} \exp\left(-\frac{E}{T}\right) \exp\left[-2\left(\frac{\theta'}{T}\right)^{1/2}\right] \exp\left(\frac{\theta}{2T}\right) \right.$$

$$+ \frac{1}{4} \int dE_p \frac{\hbar N \sigma_p}{2\pi\varepsilon_p^{5/2}} \exp\left(-\frac{4\sqrt{\theta'}}{\sqrt{\varepsilon_p} + \sqrt{\varepsilon_p + \hbar\omega}}\right)$$

$$\left. \times \int_0^\infty dE \frac{\exp\left(-E/T\right)\sqrt{2E/m}}{\sqrt{E + \hbar\omega}} \right\} = A \exp\left(\frac{\mu}{T}\right) \{I_1 + I_2\} .$$

$$(41)$$

The first term (I_1) in Eqn (41) represents the classical contribution to the mechanism of VT relaxation, which is described by the Landau – Teller dependence

$$I_1 = \int_0^\infty \frac{dE}{E + \hbar\omega} \exp\left(-\frac{E}{T}\right) \exp\left[-2\left(\frac{\theta'}{E}\right)^{1/2}\right] \exp\left(\frac{\theta}{2T}\right)$$

$$= \sqrt{\frac{4\pi}{3(\theta')^{1/2}}} E_0^{5/4} \exp\left[-3\left(\frac{\theta'}{T}\right)^{1/3}\right] \exp\left(\frac{\theta}{2T}\right) \frac{1}{E_0 + \hbar\omega}$$

$$= \sqrt{\frac{4\pi}{3}} \frac{(\theta')^{1/6} T^{5/6}}{(\theta')^{1/3} T^{2/3} + \theta} \exp\left[-3\left(\frac{\theta'}{T}\right)^{1/3}\right] \exp\left(\frac{\theta}{2T}\right) . \quad (42)$$

Here, $E_0 = (\theta')^{1/3} T^{2/3}$ is the collision energy at the saddle point of integrand in equation (42).

The second term in Eqn (41) represents the sought-for quantum correction to the molecular vibrational relaxation rate constant. The specific calculations require the energy dependence of the elastic scattering cross section for the particles engaged. Approximating this dependence by the power-like function

$$\sigma_p = \sigma(\varepsilon_0)\left(\frac{\varepsilon_0}{\varepsilon_p}\right)^{k-1/2} , \qquad \bar\sigma_p^k = \sigma(\varepsilon_0)\left(\frac{\varepsilon_0}{\theta'}\right)^{k-1/2} , \qquad (43)$$

we take the integral I_2 with the constraint $T < \theta$:

$$I_2 = \frac{1}{4} \frac{\hbar N \sigma_p^k v_T}{2\theta'} \frac{T}{\sqrt{\theta'(T + \theta)}} \frac{1}{2\sqrt{\pi}} \frac{\Gamma(2 + 2k)}{2^{1+2k}} . \qquad (44)$$

Comparison of expressions (42) and (44) is followed by the conclusion that the relative contribution of the quantum correction to the VT relaxation rate constant is given by the following relationship

$$\frac{I_2}{I_1} = \frac{1}{4} \frac{(\theta')^{1/3} T^{2/3} + \theta}{\sqrt{\theta'(T + \theta)}} \left(\frac{T}{\theta'}\right)^{1/6} \exp\left(-\frac{\theta}{2T}\right) \frac{\Gamma(2 + 2k)}{\pi 2^{2+2k}}$$

$$\times \sqrt{\frac{3}{4}} \frac{\hbar N \sigma_p^k v_T}{2\theta'} \exp\left[3\left(\frac{\theta'}{T}\right)^{1/3}\right]$$

$$\approx \frac{1}{4}\left(\frac{T}{\theta'}\right)^{1/3}\left(\frac{T}{\theta}\right)^{1/2} \exp\left(-\frac{\theta}{2T}\right) \frac{\Gamma(2 + 2k)}{\pi 2^{2+2k}}$$

$$\times \sqrt{\frac{3}{4}} \frac{\hbar N \sigma_p^k v_T}{2\theta'} \exp\left[3\left(\frac{\theta'}{T}\right)^{1/3}\right] , \qquad (45)$$

which is valid under the conditions of $T < \theta$, and $E_0 = (\theta')^{1/3} T^{2/3} \geqslant \theta$. As can be seen, this relative contribution rises linearly as the gas particle number density increases,

and under the obvious condition of $\theta \ll \theta'$ rises exponentially as the temperature decreases.

The temperature dependence of the VT relaxation rate constant can be expressed in a form convenient for further analysis:

$$k_{VT} = k_0 \left\{ \exp\left[-3\left(\frac{\theta'}{T}\right)^{1/3}\right] + C_t \right\} . \qquad (46)$$

Here, the nonexponential correction is given by the following relationship

$$C_t = \frac{1}{4}\left(\frac{T}{\theta'}\right)^{1/3}\left(\frac{T}{\theta}\right)^{1/2} \exp\left(-\frac{\theta}{2T}\right) \frac{\Gamma(2 + 2k)}{\pi 2^{2+2k}} \sqrt{\frac{3}{4}} \frac{\hbar N \sigma_p^k v_T}{2\theta'} . \qquad (47)$$

The most representative system for which the quantum correction under consideration becomes essential is the nitrogen molecule. Quite extensive experimental material has been accumulated on the subject. In this case, $m = 14 m_p$, $a = 4.55 \times 10^8$ cm^{-1}, so that the above-introduced parameters are $\theta = 3400$ K, $\theta' = 800,000$ K, and representation (46) is valid under the condition of $T > 220$ K. The factor k_0 entering formula (46) for molecular nitrogen is expressed as follows [7]:

$$k_0 = 6 \times 10^{-8} \exp\left(\frac{1690}{T}\right) T^{1/3} \exp\left(\frac{122.5}{T^{2/3}}\right) . \qquad (48)$$

The last factor in this formula accounts for the influence of the molecular attraction at low temperatures. The second term in curly brackets in Eqn (46) corresponds to the contribution from a power-like 'tail' of the particle momentum distribution function. In the case of molecular nitrogen at a temperature around room temperature, the particle elastic scattering cross sections is determined by the van der Waals interaction, according to which $k = 5/6$, and $\sigma_p \sim \varepsilon_p^{-1/3}$. This gives for nitrogen:

$$\frac{I_2}{I_1} \approx 2.9 \times 10^{-17} T^{4/3}\left(\frac{N}{N_L}\right) \exp\left(-\frac{1690}{T}\right) \exp\left(\frac{277.8}{T^{1/3}}\right) , \qquad (49)$$

where $N_L = 2.68 \times 10^{19}$ cm^{-3} is the Loschmidt number.

From the analysis performed it follows that the vibrational relaxation rate constant for diatomic molecules is represented as a sum of two terms:

$$k_{VT} = k_{cl} + k_t , \qquad (50)$$

the first of which corresponds to the classical Landau – Teller model [see the first term in formula (46) having regard to Eqn (48)], and is in quite good agreement with the experiment at temperatures higher than or on the order of 1000 K [6]. The second term constitutes the quantum correction caused by the power-like decreasing of the particle momentum distribution function. This density-dependent correction in the case of nitrogen is estimated by the following relationship

$$k_t = 1.7 \times 10^{-24} T^{5/3}\left(\frac{N}{N_L}\right) \text{ cm}^3 \text{ s}^{-1} . \qquad (51)$$

Calculations show that the relative contribution of this quantum correction at $T = 1000$ K and atmospheric pressure does not exceed a fraction of a percent. However, at
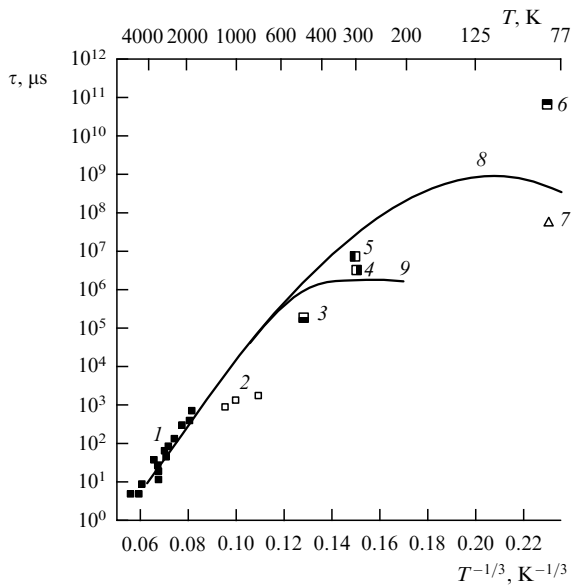
Figure 1. Temperature dependence of the vibrational–translational relaxation time at a pressure of 1 atm. The experimental points were taken from the following papers: [6] (*1*), [14] (*2*), [16] (*3*), [12] (*4*), [10] (*5*), [15] (*6*), and [17] (*7*). The line *8* represents the classical dependence corresponding to the first term in formula (50), and line *9* relates to the total VT relaxation rate constant calculated taking into account the second, quantum term in Eqn (50).

room temperature and atmospheric pressure the quantum correction $k_t(300) = 2.3 \times 10^{-20}$ cm^3 s^{-1} is about 14 times higher than that estimated from the classical Landau–Teller model: $k_{cl}(300) = 1.6 \times 10^{-21}$ cm^3 s^{-1}.

Experimental data on the vibrational–translational relaxation rate constant of the nitrogen molecule at room temperature or lower are characterized by a considerable spread of values. In this connection, one can compare the data for nitrogen at room temperature and atmospheric pressure, reported by Kovacs and Mack [12] ($k_{VT} \sim 10^{-20}$ cm^3 s^{-1}), Chatelet [9, 10] ($k_{VT} \sim 0.5 \times 10^{-20}$ cm^3 s^{-1}), and Akishev et al. [13] ($k_{VT} \sim 10^{-18}$ cm^3 s^{-1}), which differ from each other within two orders of magnitude.

Figure 1 compares the results of the theory developed here with those experimental data supplemented with the results from measurements [14–17].

One should note that the comparison of the theory with measurement data is hampered by the dependence of the vibrational relaxation rate $1/\tau_{VT} = N k_{VT}$ on the gas particle number density in the above-cited experimental works [8–10, 12] at room temperature and lower becoming nonlinear for $N \sim 10^{22}$ cm^{-3}. This magnitude of the gas density is beyond the range of applicability of the theory of interest here. The present theory predicts a deviation of the particle density dependence of the vibrational relaxation rate constant from the linear one already at atmospheric pressure and room temperature. The existing experiments relate to either atmospheric gas pressure (particle number density $N \sim 10^{19}$ cm^{-3}) or liquefied gas ($N \sim 10^{22}$ cm^{-3}) and therefore the direct comparison of the calculated density dependence of the VT relaxation rate constant with experiment is rather difficult. Such a comparison can be made after performing a direct gas phase measurement of the density dependence over a wide range of pressures, from one up to several hundred atmospheres.

One more factor bringing an uncertainty into the results obtained relates to the usage of the Lorentz gas model that assumes the mass of the scattered particle to be small compared to that of the vibrationally excited molecule. However, due to a weak sensitivity of the quantum correction to the mass of the incident particle, the usage of the model presented can hardly result in considerable error, amounting to orders of magnitude. Another source of uncertainty can be related to the usage of the power-like velocity dependence (37) of the elastic scattering cross section with the index $k = 5/6$ corresponding to the van der Waals interaction potential. Invoking a more accurate interaction potential can somewhat change the magnitude of the quantum correction.

5. The thermonuclear fusion reaction

The cross section of nonresonant thermonuclear reactions, specifically the fusion reaction

$$d + d \rightarrow t + p, \qquad (52)$$

is determined by the energy of interacting particles in the center-of-mass system (for dd-reactions, one more neutron channel exists, namely, $d + d \rightarrow He^3 + n$ having a comparable probability [18]). As was noted in Ref. [18], the main contribution to the fusion reaction at a not-too-high temperature is due to particles with energies exceeding the plasma temperature as many as several times. A considerable deviation in the energy dependence of the rate of the nonresonant fusion dd-reaction (52) from theoretical predictions was found in recent experiments [19–20]. Figure 2 shows the energy dependence of the astrophysical factor for the cross section of the fusion reaction (52), measured in experiments with the beam of deuterons interacting with deuterons incorporated into a metal crystal lattice of a target [20]. The influence of quantum effects on the rate of thermonuclear fusion reactions was considered in Refs [21, 22].

The dependence of the cross section of a reaction on the center-of-mass kinetic energy ε_p can be represented in the following form (see, e.g., Ref. [23])

$$\sigma_1(\varepsilon_p) = \frac{S(\varepsilon_p)}{\varepsilon_p} \exp\left[-2\pi\eta(\varepsilon_p)\right]. \qquad (53)$$
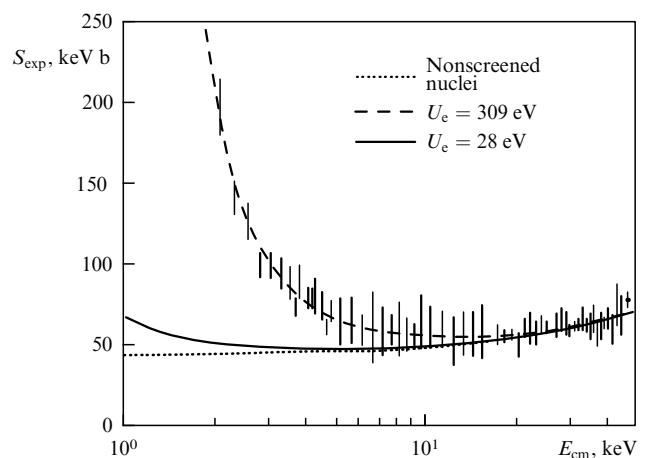

Figure 2. The beam energy dependence of the astrophysical factor for the deuteron fusion reaction cross section [20]. Experimental evidences and theoretical dependences calculated for nonscreened deuterium nuclei and nuclei screened by the free electrons of the target metal are presented.

Here, $\eta(\varepsilon_p) = Z_1 Z_2 e^2 / \hbar v$ is the Sommerfeld parameter characterizing the exponential probability of subbarrier tunneling in the Coulomb field (the Gamow factor) [4], and Z_i is the charge of the reacting particle. It is usually believed that for nonresonant reactions the astrophysical factor $S(\varepsilon_p)$ changes slightly with energy over a low-energy region. However, the measured reaction rate in a beam low-energy region $\varepsilon < 5$ keV was found to be considerably higher than the value predicted. An attempt was made to explain this effect on the basis of the hypothesis for screening ions by an electron cloud [20]. The impact of the potential U_e related to the screening of the Coulomb interaction by electrons on the reaction cross section can be accounted for in the first approximation by adding it to the collision energy [23]:

$$\sigma(\varepsilon_p) = \sigma_1(\varepsilon_p + U_e). \tag{54}$$

Since experiments [20] were performed at an enhanced density of the substance, and the above-noted contradictions between the experimental and calculated data concern a relatively low energy region, it would appear natural to explain those contradictions by the necessity of taking into consideration the quantum correction. This was tried to perform in Ref. [21] where the cross section of reaction (52), calculated with due regard for the quantum corrections to the particle momentum distribution function in the real experimental conditions, was compared with the measured data [20].

Figure 2 presents the theoretical energy dependences of the astrophysical factor obtained in that publication for non-screened deuterium nuclei and for screened ones, calculated with various magnitudes of the screening potential. As seen, the theoretical curve fits the experimental one badly at the screening potential of 28 eV that seems to be reasonable for the conditions under consideration. Good agreement in a beam low-energy region is reachable only at the screening potential of 309 eV, which is hardly a real magnitude in the conditions of the experiment. Obviously, the problems arising in interpreting the experimental results require an improvement of the theoretical models used.

A model description of fusion reactions with regard to quantum effects on the momentum distribution function in conditions of the real experiment has been presented by Coraddu et al. [21]. The reaction rate for the interaction between the beam and the target that was measured in Ref. [20] was calculated in Ref. [21]. The rate of a reaction $a + b \rightarrow c + d$ involving particles of various sorts is expressed generally as follows:

$$n_a n_b K = C \int_0^\infty \mathrm{d}E_a \int \mathrm{d}\mathbf{p}_a \int_0^\infty \mathrm{d}E_b \int \mathrm{d}\mathbf{p}_b \int \mathrm{d}\omega$$

$$\times \int \mathrm{d}q \, q^2 n_a(E_a) \left[1 \mp n_c(E_c')\right] \delta_{\gamma_a}(E_a - \varepsilon_a, \varepsilon_a)$$

$$\times n_b(E_b) \left[1 \mp n_d(E_d')\right] \delta_{\gamma_b}(E_b - \varepsilon_b, \varepsilon_b) \, \delta_{\gamma_c}(E_c' - \varepsilon_{p_c-q}, \varepsilon_{p_c-q})$$

$$\times \delta_{\gamma_d}(E_d' - \varepsilon_{p_d+q}, \varepsilon_{p_d+q}) \, \sigma_{a+b\rightarrow c+d}(\varepsilon_p) \sqrt{\frac{2\varepsilon_p}{\mu}}, \tag{55}$$

where E_a, p_a are the energy and momentum of a particle of the sort a, respectively; $E_c' = E_c + Q_c - \omega \; (E_c = E_a)$, $E_d' = E_d + Q_d + \omega \; (E_d = E_b)$; Q_i is the energy of the ith reaction product; ε_p is the center-of-mass kinetic energy of a particle; μ is the reduced mass of the colliding particles; C is the normalization factor that is to be found on the basis of

comparison with the low-density and high-temperature calculation data; $\varepsilon_{p_i} = p_i^2 / 2m_i$, and

$$\varepsilon_p = \frac{p^2}{2\mu}, \quad \text{and} \quad \mathbf{p} = \frac{m_b \mathbf{p}_a - m_a \mathbf{p}_b}{m_a + m_b}.$$

The '−' sign in Eqn (55) relates to fermions, and the '+' sign corresponds to bosons.

The magnitude of the factors $[1 \mp n(E')]$ for endothermic reactions $(Q_a < 0)$ is exponentially low. This means that the mechanism of acceleration of fusion reactions, related to the power-like tails under consideration, assumes that the plasma temperature should not be too low, as the colliding particles are already ionized, and the ionization rate is fitted by an exponential function of temperature. On the other hand, the ionization in a solid-state matrix occurs owing to the existence of the conduction electrons; however, in this case some threshold energy should also be overcome, which relates to the interaction of a deuterium ion with its surroundings in the metal.

For exothermic $(Q_a > 0)$ reactions in the nondegenerate case, the magnitude of $n(E')$ is negligible when compared to unity. The form of the expression for the occupation numbers $n(E)$ depends on the type of statistics for the system. The Bose statistics are obeyed for deuterons, so that

$$n(E) = \left[\exp\left(\frac{E - \mu}{T}\right) - 1\right]^{-1}. \tag{56}$$

The particle kinetic energy distribution function in the case of non-ideal plasma is determined by the Lorentzian

$$\delta_\gamma(E - \varepsilon, \varepsilon) = \frac{\gamma(E, \varepsilon)/\pi}{\left[E - \varepsilon - \Delta(E, \varepsilon)\right]^2 + \gamma^2}. \tag{57}$$

The linewidth is given by the following formulas [22]

$$\gamma_a(E_a, \varepsilon_a) = \hbar N \sigma_a v_a, \quad \sigma_a = \frac{\pi e^4}{\varepsilon_a^2}, \quad v_a = \sqrt{\frac{2\varepsilon_a}{m_a}}, \tag{58}$$

where N is the number density of scatters (the summation over all the scatter sorts is generally needed).

Strictly speaking, the reaction cross section involved in Eqn (55) has to be found through the solution of the quantum mechanical problem for nuclear transformation outside the mass surface. As is shown above for the case of VT relaxation, such a problem is resolvable approximately, and the final solution does not deviate considerably from that obtained by using the ordinary cross sections calculated on the mass surface. A similar approach will be applied to the case of fusion reactions, but this question, however, requires further investigation.

5w > In the case of an ideal plasma that occurs, for example, at a decreased density, the parameter $\gamma(E, \varepsilon) \rightarrow 0$. Under this conditions, the function $\delta_\gamma(E - \varepsilon, \varepsilon)$ approaches the δ function and expression (55) for the reaction rate takes the classical form. The above-presented model was utilized in Ref. [21] for numerical calculations of the reaction rates. The calculations were performed for conditions close to the experimental ones: the particle concentration $n_a = 5 \times 10^{23}$ cm^{-3}, the masses of the target (a) and projectile (b) particles $m_a = m_b = 2$ a.m.u. In the character of N involved in expression (58) for the linewidth, the concentration of scattering ions in the metal matrix was taken.

The integral (55) was calculated by the Monte Carlo method, taking account of its high dimension [21]. The particle kinetic energy distribution in the metal matrix was set to correspond to the room temperature $T = 2.44 \times 10^{-2}$ eV. The beam energy of particles of sort b was also preset.

One should note that the evaluation of the reaction rate for the beam of monoenergetic particles using Eqn (55) can be simplified, which results in the following simpler integral

$$n_a K_1 = C_1 \int_0^\infty dE_a \int d\mathbf{p}_a \int n(E_a)\, a(E_a - \varepsilon_a, \varepsilon_a) \sqrt{\frac{2\varepsilon_p}{\mu}}\, \sigma(\varepsilon_p)\,. \tag{59}$$

Here $a(E - \varepsilon, \varepsilon)$ is the Lorentzian (57). For the case of an ideal plasma, the expression for the reaction rate is simplified within the framework of this model, because the contribution of 'wings' of the Lorentz function (57) to the integral can be neglected:

$$n_a K_2 = C_2 \int_0^\infty dE_a \int d\mathbf{p}_a \int n(E_a)\, \delta(E_a - \varepsilon_a) \sqrt{\frac{2\varepsilon_p}{\mu}}\, \sigma(\varepsilon_p)$$
$$\sim \int_0^\infty d\varepsilon_a\, n(\varepsilon_a)\, \varepsilon_p \sigma(\varepsilon_p)\,. \tag{60}$$

The influence of the distribution 'tails' on the reaction rate can be evaluated comparing the results of calculations by formulas (60) and (55). These results can also be correlated with the reaction rates calculated from the relationship $K_1 = \sigma v$ using formula (53), which provides an estimation of both the factor $S(\varepsilon_p)$ and the deviation of theoretical predictions from the experiment.

In order to estimate the influence of the distribution 'tails' on the magnitude of the reaction rate (59), proper allowance must be made for the deviation of the distribution function from the Maxwellian form, which is related to a finiteness of the width of the generalized energy and momentum distribution function. As is shown in Refs [1, 3], the asymptotic expression for the kinetic energy distribution function taking into consideration the quantum correction contains the power-like dependence

$$f(\varepsilon) = C' \int_0^\infty dE_a\, n(E_a)\, a(E_a - \varepsilon_a, \varepsilon_a)$$
$$\sim \exp\left(-\frac{\varepsilon_a}{T}\right) + \frac{C_a(T)}{\varepsilon_p^4}\,. \tag{61}$$

Using this representation one can calculate the reaction rate from Eqn (59) taking into account the non-Maxwellian form of the particle kinetic energy distribution function:

$$K_3 = C_3 \int_0^\infty d\varepsilon_a\, f(\varepsilon_a) \sqrt{\frac{2\varepsilon_a \varepsilon_p}{\mu}}\, \sigma(\varepsilon_p)\,. \tag{62}$$

Table 1 shows the results of such calculations [21].

The quantities K_i outlined in Table 1 are defined by expressions (59), (60), and (62). The data in the table imply that the reaction rates calculated using different models agree well at a beam energy exceeding 2 keV. Within the energy range between 1 and 2 keV, the quantities K_1 and K_2 are close to each other, but much less than the reaction rate K. Moreover, a rather good agreement between the quantities K_3 and K should be emphasized. Therefore, one can conclude

Table 1.

E_b, keV	K_1	K_2	K_3	K	K/K_1
15	4.381×10^4	4.045×10^4	7.393×10^4	4.38×10^4	1.00
10	4.073×10^3	3.762×10^3	6.877×10^3	4.11×10^3	1.01
5	1.711×10^1	1.580×10^1	2.892×10^1	1.77×10^1	1.03
2	2.615×10^{-4}	2.421×10^{-4}	4.487×10^{-4}	2.85×10^{-4}	1.09
1.8	5.038×10^{-5}	7.223×10^{-5}	1.344×10^{-4}	5.62×10^{-5}	1.12
1.5	2.339×10^{-6}	3.850×10^{-6}	7.343×10^{-6}	3.34×10^{-6}	1.43
1.2	3.613×10^{-8}	7.474×10^{-8}	2.265×10^{-7}	7.84×10^{-7}	21.7
1	8.252×10^{-10}	7.711×10^{-10}	5.678×10^{-8}	2.82×10^{-7}	342

that the approach represented by formula (17) or (62) is quite reasonable in the order-of-magnitude estimating of the reaction rates. The results of comprehensive Monte Carlo calculations indicate a considerable contribution to the reaction rate from 'tails' in the momentum distribution function. The last column of the table contains the factor determining the deviation of the reaction rate K from that determined for the case of an ideal plasma.

Evaluation of the influence of atomic screening on the reaction rate in comparison with the above-considered mechanisms is also of interest. In doing so, the relevant calculations were performed in Ref. [21] within the framework of the model developed, setting the screening potential to $U_e = 28$ eV and taking into account its influence according to formula (54). The accepted magnitude of the screening potential seems quite reasonable for the conditions of experiment [20]. The computations imply that the screening does not notably affect the total rate of the reaction $d + d \rightarrow t + p$ studied in experiment [20] at the accepted magnitude of the potential.

It is pertinent to note that the multidimensional Monte Carlo modeling of the reaction rate, used in Ref. [21], has confirmed the reasonability of estimations performed on the basis of relationships of type (17)–(59) that where obtained within the framework of the Lorentz gas model.

One should also emphasize that the effect of the extraordinarily high fusion reaction rate is observable if there is enough time for establishing the particle momentum distribution function at high momenta. The relaxation time for the distribution function, estimated first by Galitskiĭ and Yakimets [1], is represented by the following obvious relationship

$$\tau(p) = \frac{1}{N(p/m)\, \sigma_t(p)}\,, \tag{63}$$

where $p \gg p_T$, $\sigma_t(p)$ is defined by relations of type (13), (58), and p_T is the thermal momentum of a particle. For the case of the screened Coulomb interaction, the quantity $\sigma_t(p)$ can be expressed as follows:

$$\sigma_t(p, E) = \frac{4\pi e^4}{(\varepsilon_p + E + \varepsilon_D)^2 - 4E\varepsilon_p}\,, \tag{64}$$

where $\varepsilon_D = \hbar^2/2mr_D^2$, and r_D is the Debye screening radius.

The correction to the particle momentum distribution function in a dense 'hot' plasma ($T > 1$ eV) can be estimated in the context of a Lorentz gas model in the following manner [3, 21]:

$$f(p) = \frac{1}{(2\pi mT)^{3/2}} \left[\exp\left(-\frac{\varepsilon_p}{T}\right) + \frac{\sqrt{\pi}\, N\hbar T}{\varepsilon_p^4} \sqrt{\frac{2T}{m_a}} \right]\,. \tag{65}$$

The relevant fusion reaction rate is then found from formula (55) involving the reaction cross section $\sigma_{ab}(\varepsilon_p)$. This model describes, for example, the situation where the reacting particles interact mainly with heavy admixture particles. This occurs in the experiments upon a heavy metal matrix with a particle concentration N [19, 20]. The model presented also assumes a nominally weak nonideality of the plasma and the condition $\lambda_T/l \ll 1$. It is convenient to represent the rate constant of process (52) in the form

$$k = k_{cl} + k_t. \tag{66}$$

Here, the first term

$$k_{cl} = \frac{4}{3} \sqrt{\frac{2T}{\mu}} \frac{S}{T} \tau^{1/2} \exp(-\tau) \tag{67}$$

is the classical reaction rate constant that is characterized by the astrophysical factor S [23] and the energy E_G:

$$E_G = 4 \frac{m_p}{m_e} \operatorname{Ry} z_1^2 z_2^2 \mu, \tag{68}$$

where μ is the reduced atomic mass of the particles a and b. The Gamow factor G is expressed through the energy parameters as follows [23]:

$$G = \exp\left(-\pi \sqrt{\frac{E_G}{\varepsilon_p}}\right),$$

and for the parameter τ, the following formula is valid:

$$\tau = 3 \left(\frac{\pi}{2}\right)^{2/3} \left(\frac{E_G}{T}\right)^{1/3}. \tag{69}$$

Using the above-introduced definitions one obtains the expression for the quantum correction to the rate constant of reaction (52) that depends on the medium density (cf. Refs [3, 21]):

$$k_t = \frac{4 \cdot 5!}{\pi^6} \frac{S}{E_G} \sqrt{\frac{2T}{m_a}} \frac{\hbar v}{T}. \tag{70}$$

Here, the notation was used:

$$v = \frac{N_A \rho_m e^4 \sqrt{2T/m_a}}{A_m E_G^2}. \tag{71}$$

In relationship (71), ρ_m is the density of the metal with the atomic number A_m, and N_A is the Avogadro constant. As follows from Refs [24–26], taking into account the screening effect results in an increase in the classical rate constant k_{cl} owing to the Solpeter correction f_0:

$$k'_{cl} = f_0 k_{cl}, \tag{72}$$

$$f_0 = \exp(z_1 z_2 g), \tag{73}$$

$$g = \frac{e^2}{r_D T}. \tag{74}$$

Since the above-derived expression for the quantum correction contains the integration over the kinetic energy ε_p of relative motion, the asymptotic magnitudes of which considerably exceed the screening potential U_e, the correction in question does not practically depend on the screening effect.

6. Kinetics of exothermic chemical reactions

As is well known, the rate constants of chemical reactions accompanied by the energy release usually contain the Arrhenius-like gas temperature dependence (2) [27, 28]. This means the existence of an energy barrier along the reaction coordinate, so that the relative kinetic energy of reagents has to exceed a threshold energy for carrying out their transformation into the final products. In such a case, in accordance with the concepts outlined, the magnitude of the reaction rate constant should be influenced by the quantum effects related to the occurrence of power-like 'tails' of the energy distribution function in a region of relatively low temperatures and elevated pressures. The greater part of exothermic chemical reactions in gases are characterized by a very complicated, multistage mechanism with a possible chain branching. For this reason, it is hardly possible to establish quantitatively the influence of quantum corrections to the energy distribution function on the net yield of the reaction products or the induction time in a pure form. This arises from both insufficiently reliable knowledge of parameters of all the elementary reactions, determining the rate or the characteristic time of the gross reaction, and the possible change of main reaction channels as the pressure and temperature alternate during its proceeding. Nevertheless, even the relatively simple model approach to the calculation of the kinetics of the most extensively studied reaction of hydrogen – oxygen mixture burning implies that the rate constant of this reaction can change notably at a pressure on the order of a few atmospheres as a result of inserting the quantum corrections to the particle momentum distribution function.

The rate constant of an exothermic reaction can be estimated using relations of type (14)–(17). Setting the threshold kinetic energy $\Delta E = p_0^2/2\mu$ results in

$$k_{in}(T) = \sigma_0 C \int_{p_0}^{\infty} \frac{p}{\mu} p^2 \left[\exp\left(-\frac{p^2}{2\mu T}\right) \right.$$
$$\left. + \frac{1}{2\pi} \sqrt{\frac{\pi T}{2\mu}} \frac{\hbar N T \sigma_t(p)}{\varepsilon_p^2}\right] dp. \tag{75}$$

This expression was obtained assuming the following simplified form for the momentum dependence of the reaction cross section:

$$\sigma_{in}(p) = 0, \quad p < p_0; \qquad \sigma_{in}(p) = \sigma_0, \quad p > p_0. \tag{76}$$

Besides, C is a constant responsible for the normalization of the particle energy distribution function. During computation with formula (75), the momentum dependence of the elastic scattering cross section $\sigma_t(p)$ should be specified. Approximating this dependence by the power-like function similar to Eqn (43) one obtains

$$k_{in} = \sigma_0 C \frac{p_T^4}{2} \exp\left(-\frac{\Delta E}{T}\right)$$
$$\times \left[1 + \frac{3}{4\sqrt{\pi}} \frac{v_T \hbar N \sigma_t(p_0)}{T + \Delta E} \exp\left(\frac{\Delta E}{T}\right)\right]. \tag{77}$$

In the expression obtained $p_T = (2\mu T)^{1/2}$, and $v_T = p_T/\mu$. This expression is easily transformed into the following final form convenient for further analysis:

$$k_{in} = k_0 \exp\left(-\frac{\Delta E}{T}\right) \left[1 + \frac{6.7P \exp(\Delta E/T)}{\sqrt{\mu T}(\Delta E)^{1/3}(T + \Delta E)}\right]. \tag{78}$$

Table 2. The classical magnitudes of the reaction rate constant, utilized in the numerical calculations.

No.	Reaction	$\log(A)$	b	ΔE	Q
1	$H_2 + O_2 \Rightarrow OH + OH$	13.24	0.0	48.1	-18.6
2	$OH + OH \Rightarrow H_2 + O_2$	10.82	0.3	29.2	18.6
3	$OH + H_2 \Rightarrow H + H_2O$	8.00	1.6	3.30	15.0
4	$H + H_2O \Rightarrow OH + H_2$	8.66	1.6	18.57	-15.0
5	$H + O_2 \Rightarrow OH + O$	17.08	-0.9	16.52	-16.8
6	$OH + O \Rightarrow H + O_2$	13.25	0.0	0.0	16.8
7	$O + H_2 \Rightarrow OH + H$	7.18	2.0	7.55	-1.9
8	$OH + H \Rightarrow O + H_2$	3.69	2.8	3.88	1.9
9	$H + H + M \Rightarrow H_2 + M$	17.81	-1.0	0.0	104.2
10	$H_2 + M \Rightarrow H + H + M$	18.77	-1.1	104.4	-104.2
11	$OH + H + M \Rightarrow H_2O + M$	21.92	-2.0	0.0	119.2
12	$H_2O + M \Rightarrow OH + H + M$	15.11	0.0	105.1	-119.2
13	$H + O_2 + M \Rightarrow HO_2 + M$	17.85	-0.8	0.0	46.9
14	$HO_2 + M \Rightarrow H + O_2 + M$	19.08	-1.2	48.41	-46.9
15	$HO_2 + H_2 \Rightarrow H_2O_2 + H$	13.48	0.0	26.03	-15.7
16	$H_2O_2 + H \Rightarrow HO_2 + H_2$	13.68	0.0	7.95	15.7
17	$HO_2 + HO_2 \Rightarrow H_2O_2 + O_2$	12.26	0.0	0.0	41.7
18	$H_2O_2 + O_2 \Rightarrow HO_2 + HO_2$	13.73	0.0	39.74	-41.7
19	$H + HO_2 \Rightarrow OH + OH$	14.40	0.0	1.90	38.8
20	$OH + OH \Rightarrow H + HO_2$	13.08	0.0	40.1	-38.8
21	$H + HO_2 \Rightarrow H_2O + O$	13.15	0.0	2.08	55.7
22	$H_2O + O \Rightarrow H + HO_2$	12.74	0.0	57.63	-55.7
23	$H + HO_2 \Rightarrow H_2 + O_2$	13.82	0.0	2.13	57.4
24	$H_2 + O_2 \Rightarrow H + HO_2$	14.16	0.0	56.64	-57.4
25	$O + HO_2 \Rightarrow OH + O_2$	13.24	0.0	-0.4	55.6
26	$OH + O_2 \Rightarrow O + HO_2$	13.35	0.0	52.66	-55.6
27	$OH + HO_2 \Rightarrow H_2O + O_2$	13.48	0.0	0.0	72.4
28	$H_2O + O_2 \Rightarrow OH + HO_2$	14.60	0.0	73.0	-72.4
29	$OH + OH + M \Rightarrow H_2O_2 + M$	24.70	-3.0	0.0	49.7
30	$H_2O_2 + M \Rightarrow OH + OH + M$	33.05	-4.9	53.25	-49.7
31	$HO_2 + H_2 \Rightarrow H_2O + OH$	11.78	0.0	18.68	52.4
32	$H_2O + OH \Rightarrow HO_2 + H_2$	11.44	0.0	73.74	-52.4
33	$HO_2 + H_2O \Rightarrow H_2O_2 + OH$	13.40	0.0	32.29	-30.8
34	$H_2O_2 + OH \Rightarrow HO_2 + H_2O$	13.06	0.0	1.76	30.8
35	$H + H_2O_2 \Rightarrow H_2O + OH$	13.38	0.0	3.97	68.1
36	$H_2O + OH \Rightarrow H + H_2O_2$	14.06	0.0	79.19	-68.1
37	$OH + M \Rightarrow O + H + M$	15.38	0.0	99.36	-102.3
38	$O + H + M \Rightarrow OH + M$	18.67	-1.0	0.0	102.3
39	$O + O + M \Rightarrow O_2 + M$	13.28	0.0	-1.79	119.0
40	$O_2 + M \Rightarrow O + O + M$	18.26	-1.0	118.1	-119.0
41	$O + H_2O \Rightarrow OH + OH$	10.18	1.1	17.26	-16.9
42	$OH + OH \Rightarrow O + H_2O$	9.18	1.1	0.0	16.9

Note. The temperature dependence of the rate constant was approximated by the relationship $K = AT^b \exp(-\Delta E/RT)$ (the magnitudes of rate constants for binary reactions are given in $cm^3\,mol^{-1}\,s^{-1}$ and for ternary reactions in $cm^6\,mol^{-2}\,s^{-1}$). Here, T is the temperature, K; ΔE is the activation energy, $kcal\,mol^{-1}$; Q is the energy release (energy uptake at $Q < 0$) in the same units, and M stands for a molecule in the mixture. The given reaction rate constants were found from averaging over all the components of the gas mixture.

In this relationship, $k_0 = \sigma_0 C p_T^4/2$, which corresponds to the pre-exponential factor of the reaction rate constant in the absence of the quantum correction; P is the pressure of the gaseous mixture in units of bar; μ is the reduced mass of the colliding particles in the proton mass units; ΔE is the energy defect of the reaction, and T is the gas temperature in K.

The time delay of the spontaneous combustion in hydrogen – air or hydrogen – oxygen mixtures behind the front of the reflected shock wave was studied experimentally and theoretically in Refs [29, 30]. The data obtained have shown a striking deviation (between 10 and 10^3 times) from theoretical predictions, especially utilizing pure oxygen at relatively low temperatures (~ 800 K) and elevated pressures (up to 10 MPa), with the measured time delay turned out to be much shorter than the relevant classical calculated value. Moreover, a violation of the similarity law that interconnects the spontaneous combustion time τ_i and the pressure of the mixture, $\tau_i P = $ const, has been found. The kinetic calculations of the reaction involving 42 direct and reverse processes were performed in Refs [29, 30] using the rate constants taken from Refs [31, 28].

We have done the calculations within the framework of the kinetic model [29, 30], taking account of quantum corrections in accord with the simplest approximation (78). The set of the classical rate constants used in computation is given in Table 2. The kinetic energy dependence of the elastic scattering cross section contained in formula (77) was either neglected or approximated by gas-kinetic expression (43). The most considerable influence of the quantum corrections on the magnitude of the reaction rate constant was found in the case of exothermic reactions with a high magnitude of activation energy. As an example of such a process, reaction 2 from Table 2 can be marked, the rate constant of which at a pressure of 5 atm and a temperature
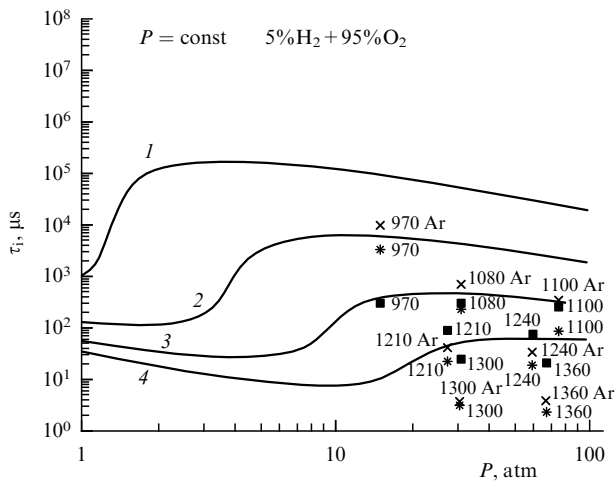
Figure 3. The pressure dependences of the spontaneous combustion time τ_i calculated and measured for various magnitudes of the initial temperature in the mixture 5% H_2 + 95% O_2. The solid lines were calculated without introducing the quantum corrections for high density to the reaction rates. The initial temperature is: 900 K (*1*), 1000 K (*2*), 1100 K (*3*), and 1200 K (*4*). The experimental points [30] are marked by black squares; the relevant initial temperature is shown alongside. The calculation results are marked by × (the temperature dependences of the reaction rate constants obey the Arrhenius law) and ∗ [the quantum corrections are taken into account with the elastic scattering cross section as given by formula (43)].
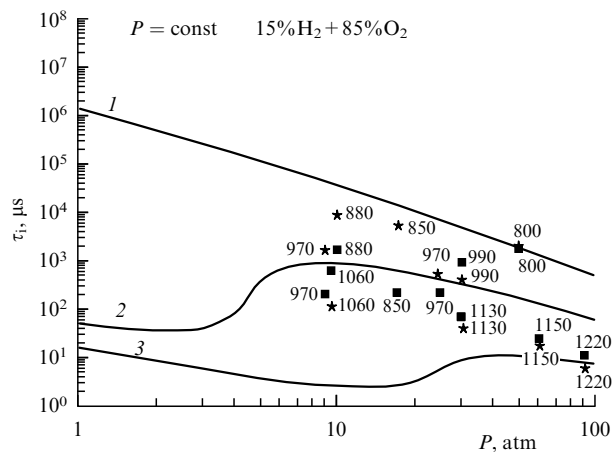

Figure 4. The pressure dependences of the spontaneous combustion time τ_i calculated and measured for various magnitudes of the initial temperature in the mixture 15% H_2 + 85% O_2. The initial temperature is: 800 K (*1*), 1000 K (*2*), and 1200 K (*3*); all the curves were obtained taking into account the quantum corrections. The experimental points [30] are marked by black squares; the relevant initial temperature is shown alongside. The data marked by ☆ were calculated making the quantum corrections. All the computations were performed neglecting the energy dependence of the particle elastic scattering cross section.

of 1000 K has increased about twice as a result of introducing the quantum correction.

The calculations were performed for two mixture compositions, as was done in Ref. [30]: (1) 5% H_2 + 95% O_2, and (2) 15% H_2 + 85% O_2. The calculated results are presented in Figs 3 and 4. The figures demonstrate that applying the quantum corrections improves the agreement with the experiment in comparison with calculations performed using the classical reaction rate constants. The agreement gets closer as the pressure rises, and the coincidence is better

when neglecting the energy dependence of the gas-kinetic collision cross section. At the same time, it would be rather naive to expect full agreement between the theory and experiment, concerning such an integral parameter as the spontaneous combustion time. This relates to the rather rough character of estimates (75) – (78) and the not fully completed model of the chemical reaction under consideration. Specifically, the existing classical model does not discriminate the rate constants of ground-state and vibrationally or electronically excited particles engaged in the reactions. Besides, other effects may show themselves in experiments, such as desorption of oxygen from the shock tube walls. However, the above-given example qualitatively testifies to a considerable contribution from the quantum corrections to kinetic calculations of chemical reactions at pressures exceeding the atmospheric pressure.

7. Quantum corrections to the nonequilibrium electron kinetic energy distribution function in a dense gas

Quantum corrections are turned out to be essential not only in the equilibrium case, as was considered in detail above, but also in a nonequilibrium situation, if the elastic collision frequency in the system is high enough. As the most widespread example of such a system we can mention weakly ionized plasma where the electron gas is found in a dense medium and subjected to the action of the external electric field. At a moderate gas pressure and low ionization degree, the electron energy distribution function (EEDF) is formed as a result of the balance of the energy and momentum of electrons which acquire the energy and momentum from the electric field and lose them in pair collisions with gas particles. Therewith, the EEDF obeys the similarity law in accordance to which the distribution function depends on the ratio of the electric field strength E to the gas particle density N [32, 33]. This law breaks down at pressures much higher than the atmospheric pressure (see, for example, Refs [34 – 39]), with the degree of deviation of the electron mobility in liquid rare gases from that determined by the similarity law amounting to several orders of magnitude, as follows from the experiments described in detail in Ref. [39]. This effect is usually explained by the increasing role of coincident collisions of an electron with several atomic particles with a rise in pressure, which causes the effective smearing of the Ramsauer minimum in the momentum transfer cross section for scattering of an electron on an atom [34]. One more possible origin of the deviation of the EEDF from the similarity law can be related to the quantum corrections to the EEDF in a dense gas, caused by a high electron – atom elastic collision frequency.

The quantum corrections indicated mainly concern the high-energy portion of the electron kinetic energy distribution function. Therefore, it is hardly expected that their introduction would change such kinetic characteristics of electrons as mobility, drift velocity, or diffusion coefficient, the magnitudes of which are governed by the electron energy of the order of its mean value. However, the magnitudes of the rate constant of electron impact excitation and ionization of gas particles in an electric field are determined by a high-energy 'tail' of the EEDF; therefore, introducing the quantum correction may turn out to be necessary in this case.

The problem of calculation of the EEDF in an electric field with due regard for the quantum corrections was stated in Ref. [40] where the case of a static electric field, as well as an

intense laser radiation field, was treated in the context of the Lorentz gas model. For some model situations, the expressions for the generalized electron energy and momentum distribution function were derived, which contained power-like decreasing dependences along with the exponential ones. The magnitude of departure from equilibrium manifests itself through the occupation numbers $n(E, p)$, while the Lorentzian characterizing spectral properties of the generalized distribution function has the form (5) (this approximation is referred to as the Kadanoff–Baym ansatz [2]).

By way of example let us consider the generalized nonequilibrium distribution function [see Eqn (5)] $f(E, \mathbf{p})$ for electrons subjected to the action of the monochromatic laser wave $E = E_L \exp(-i\omega_L t)$ [40]. Introduce the effective coefficient of electron diffusion in the space of velocities $v = p/m$:

$$D = \frac{v^2}{3} \frac{e^2 E_L^2 v_m(v)}{\omega_L^2 + v_m^2(v)} . \tag{79}$$

Here, $v_m(v)$ is the momentum relaxation frequency depending on the kinetic energy. In addition, introduce the parameter B characterizing the rate of the kinetic energy loss due to inelastic collisions (energy relaxation) with the frequency $v_\varepsilon(v)$:

$$B = ETv_\varepsilon(v) , \tag{80}$$

where T is the gas temperature. Then we obtain the following expression for the occupation numbers [40]:

$$n(E, p) = \left[\exp\left(\int_0^E \frac{d\varepsilon}{T} \frac{B}{D + B} - \frac{\mu}{T} \right) + 1 \right]^{-1} , \tag{81}$$

which transforms into the Fermi distribution (6) in the low-field limiting case $(D \ll B)$. In the opposite limiting case $D \gg B$, corresponding to a strongly nonequilibrium situation, the asymptotic estimation of behavior of the electron momentum distribution function can be realized assuming power-like velocity dependences of frequencies of elastic and inelastic electron–molecule collisions: $v_m(v) \sim v^l$, $v_\varepsilon(v) \sim v^{l+q}$ (l, q are the fitting parameters for these dependences). In the limit $\omega_L \gg v_m$, this leads to the following dependence [3]:

$$f(p) \propto p^{-(26+3q)/4} . \tag{82}$$

The above-outlined approach was applied in Ref. [40] for estimating the rate constants of inelastic electron–molecule collisions. Specifically, it is shown that introducing the quantum correction results in a drastic (about five orders of magnitude) increase in the electron-impact atomic ionization rate constant.

Note one more effect showing itself in nonideal plasma and promoting an increase in the excitation and ionization rate constants. This relates to the Debye screening, resulting in an effective lowering of the ionization potential of atoms or ions in plasma. The phenomenon is similar to the Solpeter effect [see formulas (72)–(74)] consisting in an increase of the fusion reaction rate due to the screening of the Coulomb interaction in plasma. This effect was explored in Refs [41–46] in application to the problems of radiation and collision kinetics of equilibrium and nonequilibrium classical plasmas. The calculations performed in Ref. [47] under the same assumptions and with the introduction of the quantum correction into the electron energy distribution function showed that the latter effects resulted in an ionization rate constant exceeding by an order of magnitude that which takes into account the screening effect. Moreover, the screening effect becomes notable at a large magnitude of the plasma nonideality factor, while the expressions derived in Refs [41–46] are valid, strictly speaking, in the limit of a weak nonideality.

8. Conclusions

The examples given above imply a notable influence of quantum effects upon the particle momentum distribution function; occurrence of power-like asymptotic dependences ('tails') at high kinetic energies affects the rates of threshold or barrier exothermic reactions. Examples of such an influence and comparison with the available experimental data confirm, at least qualitatively, the importance of the quantum effects in VT relaxation processes, thermonuclear fusion reactions, and chemical transformations. The quantitative evaluation of the rate constants of those processes with due regard for the quantum effects requires, on the one hand, developing the more accurate numerical models involving the real energy dependences of both elastic and inelastic collision processes and, on the other hand, improving the experimental methods for studying inelastic processes at elevated pressures. It should be recognized that the key point in the theoretical approach applied is the scattering amplitude outside the mass surface, which determines the cross sections of elementary processes and comprises a new object of theoretical and experimental research that has not been adequately explored up to now. The aim of this article is to focus attention on the importance of this object and stress some problems arising from its study.

References

1. Galitskiĭ V M, Yakimets V V *Zh. Eksp. Teor. Fiz.* **51** 957 (1966) [*Sov. Phys. JETP* **24** 637 (1967)]
2. Kadanoff L P, Baym G *Quantum Statistical Mechanics* (New York: W.A. Benjamin, 1962) [Translated into Russian (Moscow: Mir, 1964)]
3. Starostin A N et al. *Physica A* **305** 287 (2002)
4. Landau L D, Lifshitz E M *Kvantovaya Mekhanika: Nerelyativists-kaya Teoriya* (Quantum Mechanics: Non-Relativistic Theory) (Moscow: Fizmatlit, 1963) [Translated into English (Oxford: Pergamon Press, 1965)
5. Landau L D, Teller E, in *Sobranie Trudov L.D. Landau* (Collected Works) Vol. 1 (Moscow: Nauka, 1969) p. 181; *Phys. Z. Sowjetunion* **10** 34 (1936)
6. Millikan R C, White D R *J. Chem. Phys.* **39** 98 (1963)
7. Gordiets B F, Osipov A I, Shelepin L A *Kineticheskie Protsessy v Gazakh i Molekulyarnye Lazery* (Kinetic Processes in Gases and Molecular Lasers) (Moscow: Nauka, 1980) [Translated into English (New York: Gordon and Breach Sci. Publ., 1988)]
8. Chateau M et al. *J. Chem. Phys.* **71** 4799 (1979)
9. Chatelet M et al. *J. Chem. Phys.* **75** 2374 (1981)
10. Chatelet M, Chesnoy J *Chem. Phys. Lett.* **122** 550 (1985)
11. Jackson J H, Mott N F *Proc. R. Soc. London Ser. A* **137** 703 (1932)

12. Kovacs M A, Mack M E *Appl. Phys. Lett.* **20** 487 (1972)
13. Akishev Yu S et al. *Teplofiz. Vys. Temp.* **20** 818 (1982) [*High Temp.* **20** 658 (1982)]
14. Lukasik S J, Young J E *J. Chem. Phys.* **27** 1149 (1957)
15. Chandler D W, Ewig G E *J. Chem. Phys.* **73** 4904 (1980)
16. Henderson M C *J. Acoust. Soc. Am.* **34** 349 (1962)
17. Brueck S R G, Osgood R M *Chem. Phys. Lett.* **39** 569 (1976)
18. Artsimovich L A *Upravlyaemye Termoyadernye Reaktsii* (Controlled Thermonuclear Reactions) (Moscow: Nauka, 1961) [Translated into English (New York: Gordon and Breach Sci. Publ., 1964)]
19. Raiola F et al. *Phys. Lett. B* **547** 193 (2002)
20. Raiola F et al. *Eur. Phys. J. A* **13** 377 (2002)
21. Coraddu M et al. *Physica A* **340** 490, 496 (2004)
22. Starostin A N, Savchenko V I, Fish N J *Phys. Lett. A* **274** 64 (2000)
23. Ichimaru S *Rev. Mod. Phys.* **65** 255 (1993)
24. Salpeter E E *Austr. J. Phys.* **7** 373 (1954)
25. Brown L S, Sawyer R F *Rev. Mod. Phys.* **69** 411 (1997)
26. Bahcall J N et al. *Astron. Astrophys.* **383** 291 (2002)
27. Kondrat'ev V N, Nikitin E E *Kinetika i Mekhanizm Gazofaznykh Reaktsiĭ* (Kinetics and Mechanisms of Gas Phase Reactions) (Moscow: Nauka, 1974)
28. Warnatz J, Maas U, Dibble R W *Combustion: Physical and Chemical Fundamentals, Modeling and Simulation, Experiments, Pollutant Formation* 3rd ed. (Berlin: Springer-Verlag, 2001) [Translated into Russian (Moscow: Fizmatlit, 2003)]
29. Gel'fand B E et al. *Dokl. Ross. Akad. Nauk* **330** 457 (1993) [*Dokl. Phys. Chem.* **330** 260 (1993)]
30. Gel'fand B E et al. *Dokl. Ross. Akad. Nauk* **349** 482 (1996) [*Dokl. Phys. Chem.* **349** 183 (1996)]
31. Tsang W, Hampson R *J. Phys. Chem. Ref. Data* **15** 1087 (1986)
32. Ginzburg V L *Rasprostranenie Elektromagnitnykh Voln v Plazme* (The Propagation of Electromagnetic Waves in Plasmas) (Moscow: Nauka, 1965) [Translated into English (Oxford: Pergamon Press, 1970)]
33. Smirnov B M *Fizika Slaboionizovannogo Gaza v Zadachakh s Resheniyami* (Physics of Weakly Ionized Gases: Problems and Solutions) (Moscow: Nauka, 1985) [Translated into English: *Physics of Ionized Gases* (New York: Wiley, 2001)]
34. Khrapak A G, Yakubov I T *Elektrony v Plotnykh Gazakh i Plazme* (Electrons in Dense Gases and Plasma) (Moscow: Nauka, 1981)
35. Smirnov B M *Usp. Fiz. Nauk* **172** 1411 (2002) [*Phys. Usp.* **45** 1251 (2002)]
36. Gordon E B, Rzhevskiĭ O S, Khmelenko V V *Kvantovaya Elektron.* **21** 209 (1994) [*Quantum Electron.* **24** 191 (1994)]
37. Gordon E B, Khmelenko V V, Rzhevsky O S *Chem. Phys. Lett.* **217** 605 (1994)
38. Gordon E B, Shestakov A F *Fiz. Nizk. Temp.* **27** 1192 (2001) [*J. Low Temp. Phys.* **27** 883 (2001)]
39. Gordon E B, Smirnov B M *Zh. Eksp. Teor. Fiz.* **125** 1058 (2004) [*JETP* **98** 924 (2004)]
40. Starostin A N et al. *Contribut. Plasma Phys.* **39** 93 (1999); Starostin A N *Contribut. Plasma Phys.* **41** 299 (2001)
41. Schlanges M, Bornath Th, Kremp D *Phys. Rev. A* **38** 2174 (1988)
42. Bornath Th, Schlanges M, Kremp D *Contribut. Plasma Phys.* **28** 57 (1988)
43. Klimontovich Yu L, Schlanges M, Bornath Th *Contribut. Plasma Phys.* **30** 349 (1990)
44. Schlanges M, Bornath Th, Kremp D, in *Physics of Nonideal Plasmas* (Teubner-Texte zur Physik, Bd. 26, Eds W Ebeling, A Förster, R Radtke) (Stuttgart: B.G. Teubner Verlagsgesellschaft, 1992) p. 154
45. Kremp D et al. *Phys. Rev. E* **47** 635 (1993)
46. Atrazhev V M, Iakubov I T, Roldughin V I *J. Phys. D: Appl. Phys.* **9** 1735 (1976)
47. Aleksandrov N L, Starostin A N *Zh. Eksp. Teor. Fiz.* **113** 1661 (1998) [*JETP* **86** 903 (1998)]